

---

# Demonstration of Dual-Tripler, Broadband Third-Harmonic Generation and Implications for OMEGA and the NIF

A critical concern for Nd:glass fusion lasers such as OMEGA and the National Ignition Facility (NIF) is the uniformity of irradiation experienced by the fusion target. Uniform beams are generated by beam-smoothing schemes such as smoothing by spectral dispersion (SSD),<sup>1</sup> which vary the instantaneous speckle pattern on target on time scales that are short compared with relevant hydrodynamic time scales. In a simplified picture of beam smoothing, the laser presents a new speckle pattern to the target every coherence time, where the coherence time is given by the inverse of the bandwidth. The beam is smoothed because the target responds hydrodynamically to the average of a large number of independent speckle patterns. The ratio of the coherence time to the relevant hydrodynamic time is thus a key parameter. Alternatively stated, the time required to obtain a given level of uniformity is inversely proportional to the laser bandwidth.

Smoothing achieved using present fusion lasers is limited by the bandwidth acceptance of the KDP crystals that are used for third-harmonic generation (THG). Conventionally, THG involves frequency doubling in a first, “doubler” crystal followed by sum-frequency mixing in a second, “tripler” crystal.<sup>2</sup> Eimerl *et al.*<sup>3</sup> recently proposed, however, that broader-bandwidth THG can be achieved by using dual triplers, i.e., two tripler crystals in series with slightly different angular detunings from phase matching and appropriately chosen thicknesses. Oskoui<sup>4</sup> showed that by adding a second tripler to the existing conversion crystals in each beamline of the OMEGA laser system it is possible to increase the bandwidth acceptance by a factor of 3, and he developed an optimized design. Conversion of OMEGA to dual-tripler THG is now underway.

This article reports on what is believed to be the first experimental demonstration of dual-tripler THG. A second (type-II) KDP tripler, with 9-mm thickness, was added to a tripling cell (used on the former 24-beam OMEGA laser system) containing two type-II, 16-mm KDP crystals. All crystals were antireflection coated. The dual-tripler configuration was tested using a narrow-bandwidth, high-power laser beam whose angle of incidence on the crystals was varied. The

THG conversion efficiency was measured as a function of this angle. Since an angular tilt of the incident IR beam is equivalent to a change in its wavelength (this relationship is linear to a good approximation, with  $\sim -160 \mu\text{rad}$  equivalent to  $1 \text{ \AA}^5$ ), a measured increase in the angular acceptance of the THG conversion is equivalent to a proportional increase in the THG acceptance bandwidth.

One important parameter investigated in the experiment was the separation between the two triplers. The relative phase  $\Delta\Phi$  between the three interacting waves (defined as  $\Delta\Phi = \Phi_3 - \Phi_2 - \Phi_1$ , where  $\Phi_i$  is the phase of harmonic  $i$ ) can change due to a number of factors, including dispersion in the air path between the triplers, dispersion in the windows of the crystal cell, and phase changes due to the coatings on the crystal surfaces. (The relative phase within a tuned crystal is zero by the definition of phase matching.) Using the formula  $(n-1) \times 10^7 = 2726.43 + 12.288/\lambda^2 + 0.3555/\lambda^4$ , where  $n$  is the refractive index and the wavelength  $\lambda$  is in  $\mu\text{m}$ ,<sup>6</sup> 4.0 cm of air is predicted to be equivalent to a full cycle of phase shift [i.e.,  $(k_3 - k_2 - k_1)L = 2\pi$ , where  $k_i$  is the wave vector in air of harmonic  $i$  and  $L = 4 \text{ cm}$ ]. In the experiment, the relative phase  $\Delta\Phi$  emerging from the first tripler was unknown due to dispersion in the output cell window; thus, to ensure the optimum  $\Delta\Phi$  at the input to the second tripler, it was necessary to adjust the air gap to the optimum position within this 4-cm range.

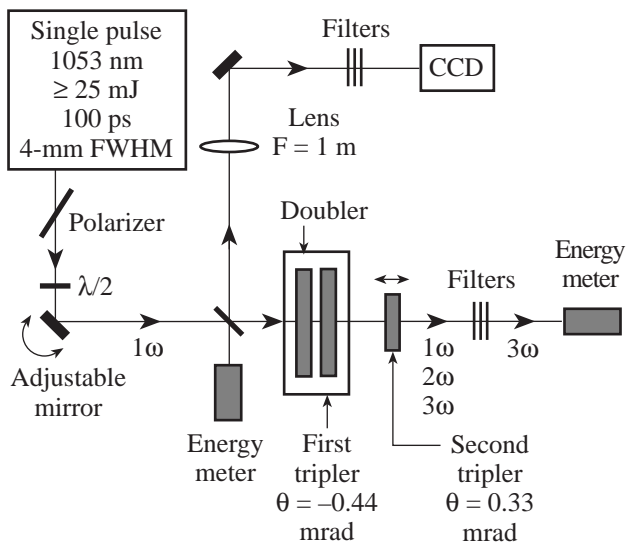
This article extends the work of Ref. 7, which reports the experimental results, to include details of the dual-tripler design currently being implemented on OMEGA and a dual-tripler design that could provide a comparable bandwidth on the NIF.

## Experiment

The laser beam used in the experiment originated from a Nd:YLF-based, diode-pumped, mode-locked oscillator that generated a train of bandwidth-limited, 100-ps-duration pulses. A single pulse was switched out and amplified in a flash-lamp-pumped, negative-feedback-controlled, regenerative amplifier<sup>8</sup> and two subsequent single-pass, flash-lamp-

pumped, Nd:YLF amplifiers separated by spatial filters. This produced a collimated beam with 100-ps time duration, up to 25 mJ of energy, and an approximately Gaussian spatial profile with a FWHM diameter of 4 mm.

The experimental setup is shown in Fig. 75.1. The input laser beam was reflected off an adjustable mirror, which was used to vary its angle of incidence on the crystals. Back-reflections from the crystal surfaces were transported through a 1-m focus lens onto a CCD camera to monitor the beam alignment relative to the crystals and the relative alignment between the crystals. The polarization of the incoming beam was adjusted using a half-wave plate to be  $35^\circ$  with respect to the  $o$  axis of the first crystal. The second tripler was mounted on a stage with a 5-cm translation range, which was required to optimize the relative phase between the three interacting waves incident on the second tripler. The crystals were set up using the converging-lens technique<sup>9</sup> with a separation of  $\sim 0.77$  mrad between the phase-matching directions of the two triplers, this angle being the optimum predicted separation.



E8928

Figure 75.1  
Experimental setup.

The experimental results are shown in Fig. 75.2 for five values of the air gap spanning the 4-cm range in 1-cm increments. The results are in excellent agreement with predictions of the plane-wave code Mixette (based on Ref. 2), which calculates the conversion averaged over the assumed Gaussian spatial and temporal beam profiles at a nominal intensity of  $1.2 \text{ GW/cm}^2$ .

The conversion efficiency was measured as the ratio of the energy of the third-harmonic beam at the output of the second tripler to the energy of the fundamental beam at the input to the doubler. For each angular position several measurements (typically 5 to 7) were made, and the averaged value was used as the measured conversion efficiency. Typically the averaged data had an uncertainty (standard deviation) of the order of 1% or less, although in a few cases the uncertainty was as large as  $\sim 5\%$ .

Small scaling factors were applied to the experimental measurements (0.95 to the angle and 1.04 to the conversion) to account for systematic uncertainties in the accuracies with which the values of angles and intensities were measured. These scaling factors were determined from one data set and were then maintained constant for the remainder of the experiment. The calculations assumed that the first tripler was detuned to be phase matched for a beam tilt of  $-0.44$  mrad on the horizontal axes of Fig. 75.2. The corresponding tilt for the second tripler was  $0.33$  mrad, all tilt angles quoted in this article being external to the crystals. (The absolute values of these angles were not known experimentally.) The optimum air gap [corresponding to Figs. 75.2(a) and 75.2(e)] was assumed to be 1.5 cm away from the point of no net dispersion [midway between that in Figs. 75.2(c) and 75.2(d)]. The sign of this distance depends on the orientations of the optic axes of the triplers, which were parallel in this experiment. The calculations shown in Fig. 75.2 assumed a 4.1-cm period, which was found to fit the data slightly better than the predicted 4.0-cm period; this small difference is ascribed to different temperatures, humidity, etc., from those of Ref. 6.

The nominal laser intensity  $I_{\text{nom}}$ , defined as

$$E / (\pi r_{\text{HW}}^2 \tau_{\text{FWHM}}),$$

where  $E$  is the laser energy and  $2r_{\text{HW}}$  and  $\tau_{\text{FWHM}}$  are the spatial and temporal FWHM's, respectively, was  $1.2 \text{ GW/cm}^2$ , corresponding to a peak intensity in space and time of  $0.78 \text{ GW/cm}^2$ . The low conversion efficiencies shown in Fig. 75.2 are primarily a result of the non-optimum beam profile (Gaussian in both space and time), for which 50% of the IR energy is incident at less than 30% of the peak intensity. This is illustrated in Fig. 75.3, which reproduces the data and calculated curve of Fig. 75.2(e) and adds predictions for what would have been obtained with different beam spatial and temporal profiles. It is seen that conversion efficiencies up to 80% would have resulted for beams flat in space and time.

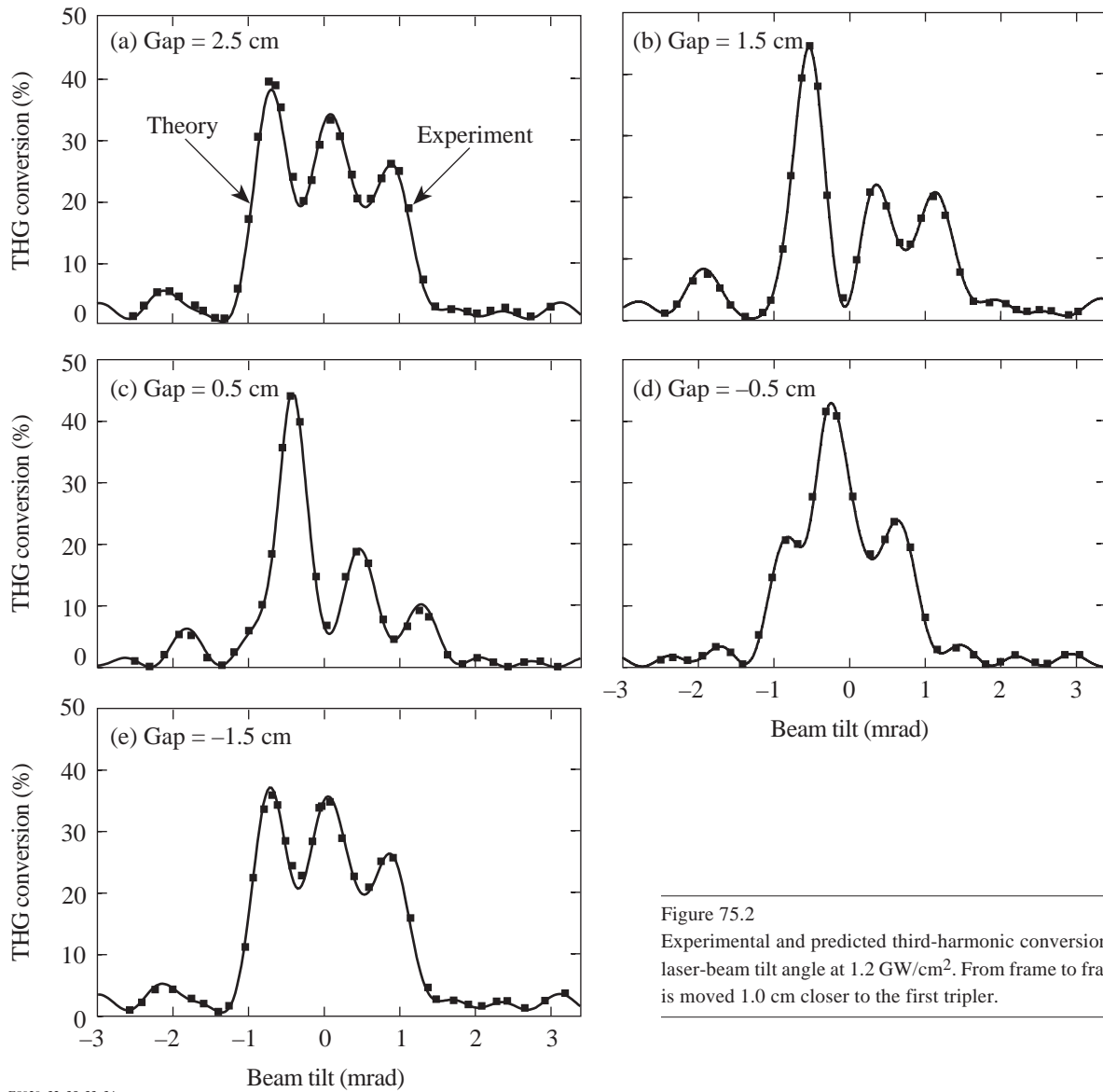


Figure 75.2  
Experimental and predicted third-harmonic conversion as a function of the laser-beam tilt angle at  $1.2 \text{ GW/cm}^2$ . From frame to frame the second tripler is moved 1.0 cm closer to the first tripler.

E8929, 32, 35, 33, 34

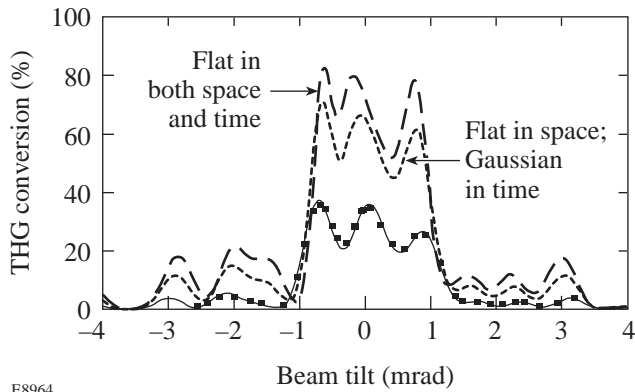
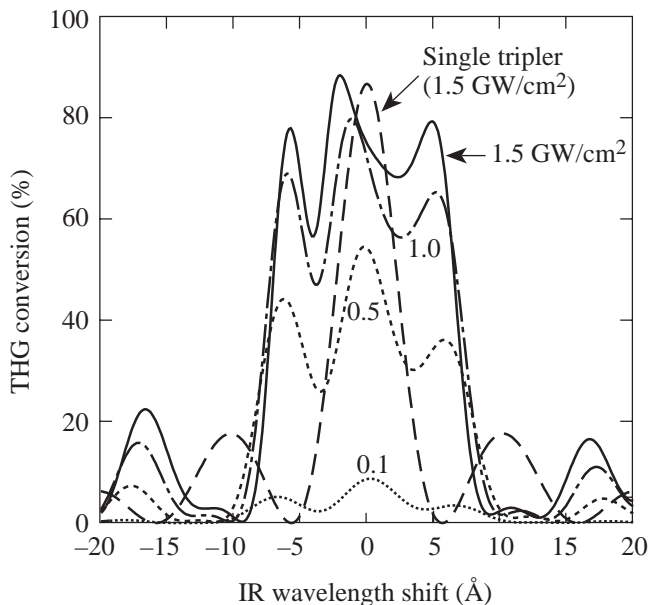


Figure 75.3  
THG conversion versus beam tilt angle for the conditions of Fig. 75.2(e) (solid curve and data points) together with predictions for what would have been obtained if the beam were flat in space but Gaussian in time (dotted curve) and flat in both space and time (dashed curve). All curves are for a nominal intensity of  $1.2 \text{ GW/cm}^2$ .

E8964

### Design for OMEGA

Figure 75.4 shows predictions for single rays (i.e., beams that are flat in space and time) for the OMEGA laser system, assuming that an 8-mm tripler crystal is added to each beam after the existing conversion crystals (which are both 12.2-mm, type-II KDP crystals). Here the first tripler is detuned 0.62 mrad (to phase match at  $-3.84 \text{ \AA}$ ), and the second is detuned  $-0.38 \text{ mrad}$  (to phase match at  $2.36 \text{ \AA}$ ). The air gap is 1.0 cm. Curves are shown for intensities from 0.5 to  $1.5 \text{ GW/cm}^2$ , spanning the range of normal operating conditions, and for small signal ( $0.1 \text{ GW/cm}^2$ ). At  $1.5 \text{ GW/cm}^2$ , the FWHM bandwidth is  $13.8 \text{ \AA}$ , corresponding to  $1.1 \text{ THz}$  at  $351 \text{ nm}$ , and at lower intensities the bandwidth is slightly greater.



TC4624

Figure 75.4

Predicted performance of the OMEGA laser system as a function of IR wavelength shift, for the addition of a second tripler of 8-mm thickness at a separation of 1.0 cm. The curves correspond to intensities ranging from 1.5 to  $0.1 \text{ GW/cm}^2$ . The dashed curve corresponds to the existing system at  $1.5 \text{ GW/cm}^2$ . At this intensity, the extra tripler increases the FWHM bandwidth from  $4.9 \text{ \AA}$  to  $13.8 \text{ \AA}$  ( $1.1 \text{ THz}$  in the UV). The curves in this and similar figures are calculated for monochromatic beams with varying wavelength.

The shape of the dual-tripler curve at  $1.5 \text{ GW/cm}^2$  is advantageous for the conversion of a broad-bandwidth phase-modulated beam. The THG conversion is maintained in the 60%–90% range as the IR wavelength varies through  $\pm 6 \text{ \AA}$ . In contrast, the single-tripler curve results in significant loss beyond  $\pm 2 \text{ \AA}$ . In a typical SSD laser beam, the instantaneous wavelength will vary in time through  $\pm 6 \text{ \AA}$  at any point in the

beam cross section, and, at each time, it will exhibit a similar variation across the beam aperture. The net conversion integrated over the beam will then correspond to some average over wavelength of the curves of Fig. 75.4, depending on the specific parameters of the SSD design used.

The dual-tripler design being implemented on OMEGA calls for the triplers to be spaced 1.0 cm apart with a tolerance of  $\pm 0.1 \text{ cm}$ , and for their relative angular separation to be accurate within  $100 \text{ \mu rad}$ . Curves illustrating the effects of these deviations are shown in Fig. 75.5 for the peak anticipated operating intensity of  $1.5 \text{ GW/cm}^2$ . In both cases, the variations in the predicted conversion curves are considered acceptable. The variations experienced in the spatially averaged conversion efficiency will be less (of the order of 1%–2%) because the curves resulting from deviations from the design lie above the design at some wavelengths and below the design at others.

It is worth noting that the alignment accuracy required by dual-tripler THG is no greater than that already in place on OMEGA. Currently the crystals are tuned to a much smaller tolerance than  $100 \text{ \mu rad}$ .

### Design for the NIF

Very similar broadband conversion may also be obtained on the NIF. Two designs are considered here (see Table 75.I): The “11/8/10” design was suggested in Ref. 3, although with slightly different tuning angles. (It should be noted that all angles quoted in Ref. 3 are internal to the crystal, i.e., 1.5 times smaller than the external angles quoted here.) The “11/9/9” design is an alternative design that is compatible with the NIF two-crystal base-line design (“11/9”).

A comparison between the two dual-tripler designs is shown in Fig. 75.6. The “11/8/10” design provides slightly more conversion and allows slightly more bandwidth; otherwise, the two designs are very similar. The curves are remarkably similar to those of the optimum OMEGA design of Fig. 75.4; again, the range of wavelengths that can be efficiently converted is increased from  $\pm 2 \text{ \AA}$  to  $\pm 6 \text{ \AA}$ .

Comparing either dual-tripler design with the two-crystal base-line design, shown superposed on both plots of Fig. 75.6 at the nominal operating intensity of  $3.0 \text{ GW/cm}^2$ , it is clear that there will be some loss in overall conversion when averaging over a broadband beam, but probably no more than 10% based on the  $3.0\text{-GW/cm}^2$  curve. (The loss at lower intensities is less.)

The effective beam uniformity resulting from dual-tripler conversion on the NIF may be even greater than that on OMEGA, based on the reasonable presumption that it is the ratio between the coherence time (1/bandwidth) and the rel-

evant hydrodynamic time that is important. The coherence time is the same on each system, but the hydrodynamic time scales are a few times longer on the NIF.

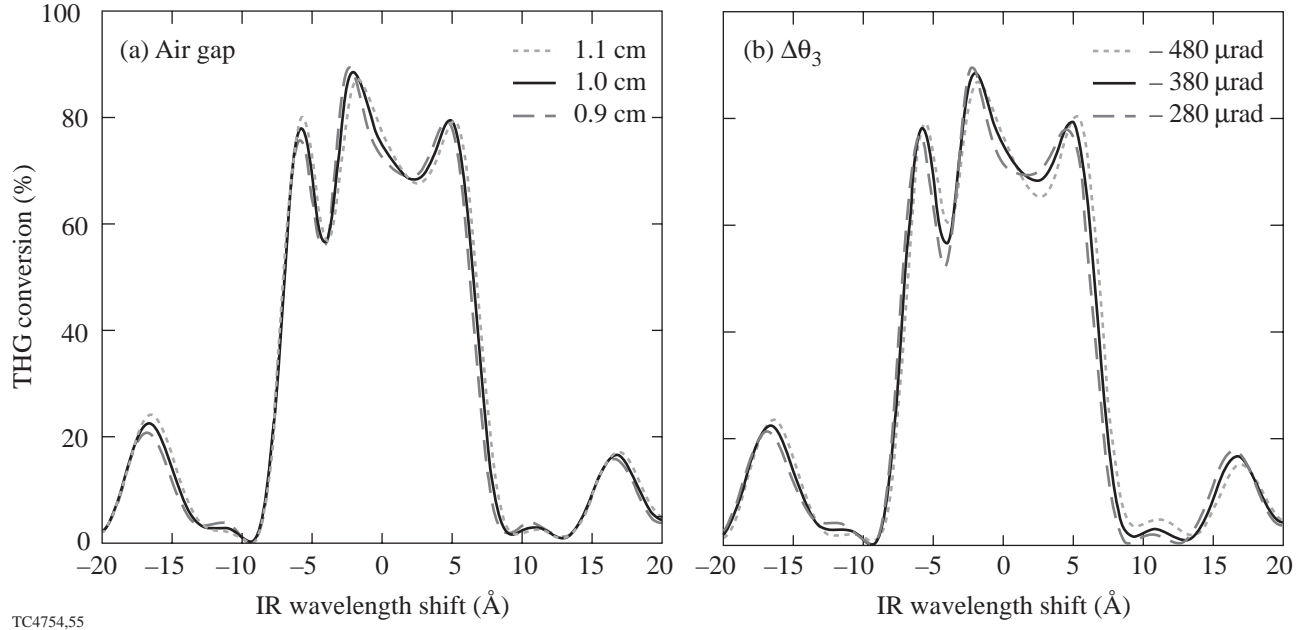


Figure 75.5 Sensitivity of the base-line design for dual-tripler THG on OMEGA to (a) deviations in the air gap between triplers from 1.0 cm and (b) deviations in the tilt angle of the second tripler from  $-380 \mu\text{rad}$ . All curves are for the maximum anticipated operating intensity of  $1.5 \text{ GW}/\text{cm}^2$ . Deviations of no greater than (a)  $\pm 0.1 \text{ cm}$  and (b)  $\pm 100 \mu\text{rad}$  are acceptable.

Table 75.I: Existing and dual-tripler designs for OMEGA and the NIF. Tilt angles  $\Delta\theta_i$  are external to the crystals, with a positive angle indicating an increase in the angle between the propagation direction and the optic axis. OMEGA crystals are all type-II KDP; NIF doublers are type-I KDP and triplers type-II KD\*P. Subscript “1” indicates the doubler, “2” the first tripler, and “3” the second tripler.

	Crystal thickness (mm)			Crystal tilt ( $\mu\text{rad}$ )			Gap between triplers (mm)
	$L_1$	$L_2$	$L_3$	$\Delta\theta_1$	$\Delta\theta_2$	$\Delta\theta_3$	gap
OMEGA, present	12	12	–	0	0	–	–
OMEGA, dual tripler	12	12	8	0	620	$-380$	10
NIF “11/9” base line	11	9	–	350	0	–	–
NIF “11/8/10”	11	8	10	325	900	$-1000$	0
NIF “11/9/9”	11	9	9	325	750	$-1000$	0

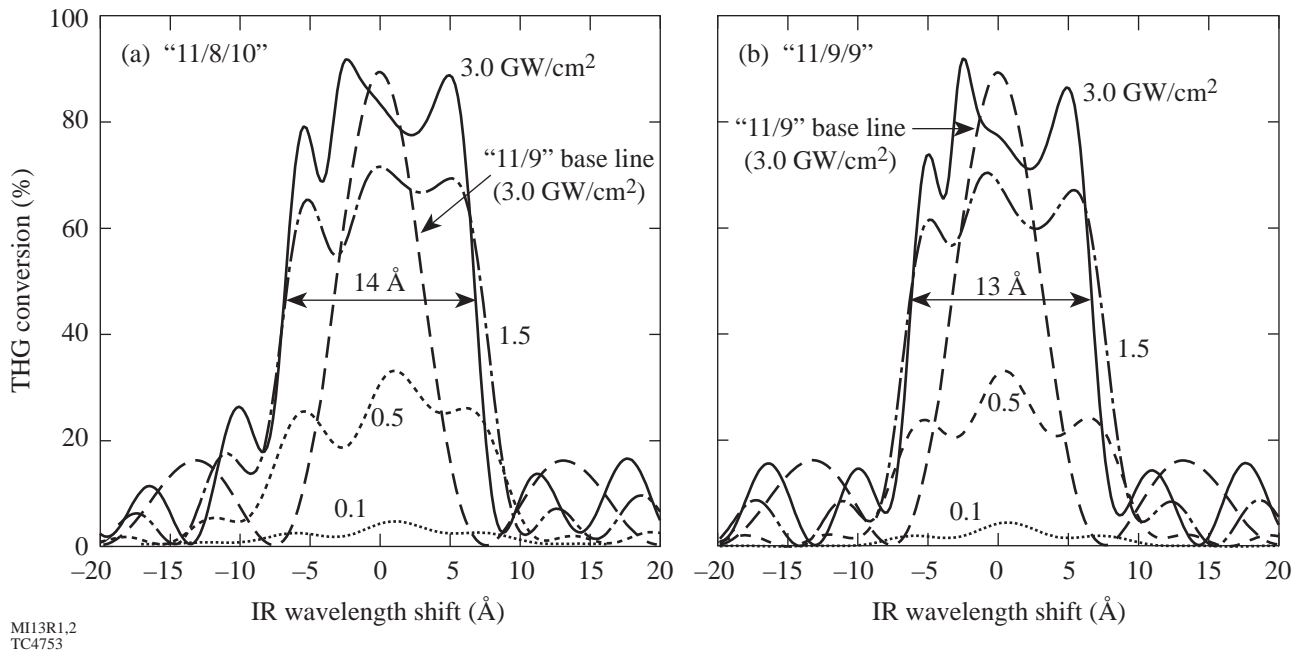


Figure 75.6

Predicted performance for two enhanced-bandwidth designs for the NIF: (a) the “11/8/10” design of Eimerl (Ref. 3) and (b) an alternative “11/9/9” design that leaves the base-line, two-crystal, “11/9” NIF design unchanged.

One important difference between OMEGA and the NIF is that the optimum “11/8/10” and “11/9/9” designs for the NIF require no relative phase change between the triplers. This will indeed be the case on the NIF since the base-line design calls for the crystals to be mounted in vacuum. It is anticipated that the antireflection (AR) coatings on the output of the first tripler and the input to the second tripler will not significantly affect the phase at any wavelength.

Transmission losses between crystal surfaces have not been included in the calculations presented here for OMEGA and the NIF since the AR coatings have not yet been designed. Small losses will be incurred since one cannot simultaneously eliminate reflections at all three wavelengths; however, this does not significantly affect the results presented here.

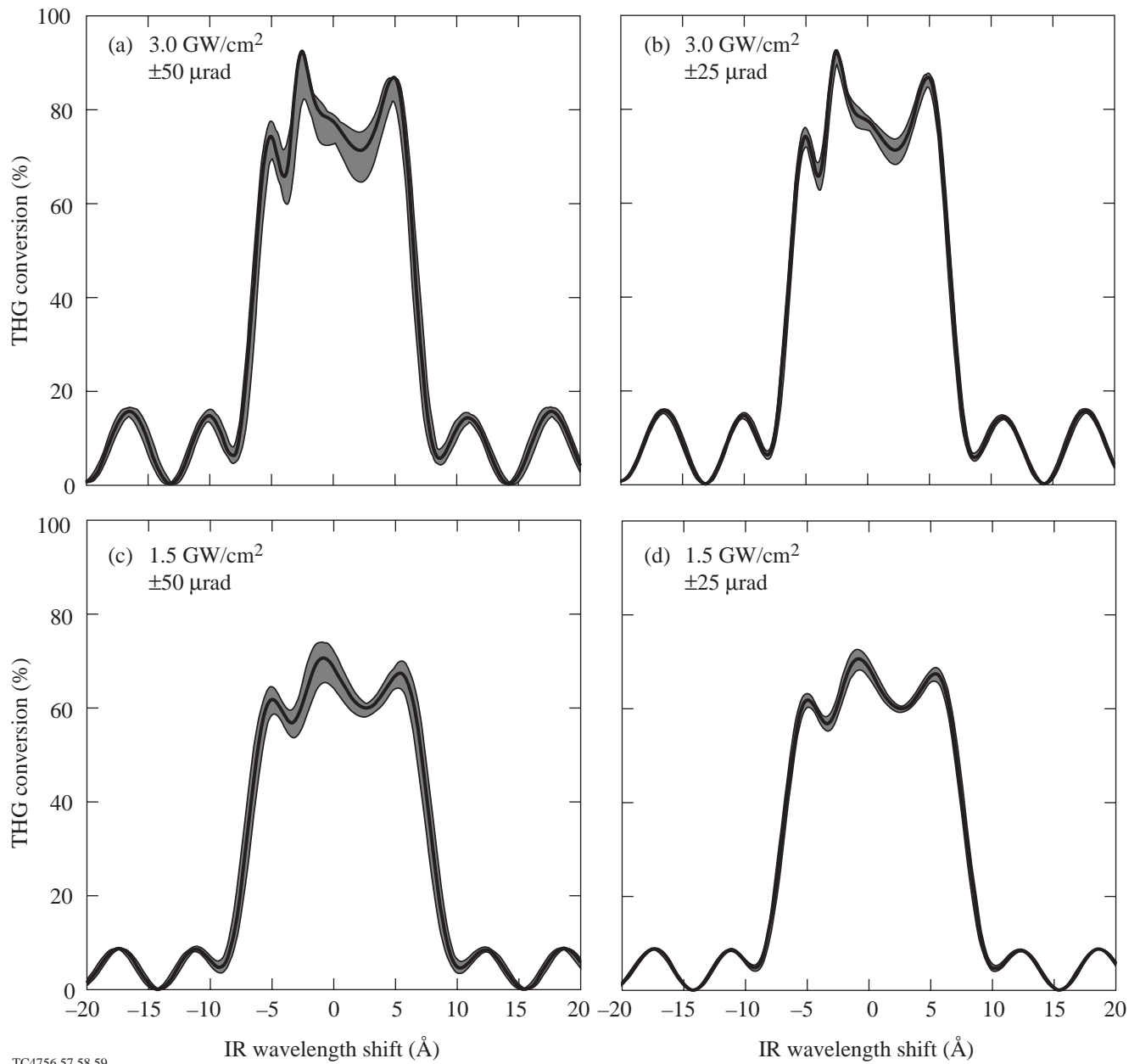
The sensitivity of the “11/9/9” dual-tripler design for the NIF to angular misalignments of the crystals is shown in Fig. 75.7. In each case, the ideal conversion curve was calculated together with eight variants. In each variant, each crystal was tilted by either  $+\Delta\theta$  or  $-\Delta\theta$ . The shaded areas on the plots indicate the envelope of all eight of these variants, including the worst-case combinations. Again, less variation may occur in some cases for the average over a broadband

beam since some curves lie below ideal at some wavelengths and above ideal at others. Results for a tolerance of  $\pm 25 \mu\text{rad}$  are clearly better than those for  $\pm 50 \mu\text{rad}$ .

At  $1.5 \text{ GW/cm}^2$ , the greatest deviations from ideal occur as a result of detunings of the doubler from the design orientation. These deviations are essentially the same that occur for the base-line, two-crystal NIF design and result from the sensitivity of the angle-detuned, type-I/type-II design to doubler orientation;<sup>2</sup> thus, the addition of a second tripler to the NIF does not require any greater angular alignment accuracy than is already included in the base-line design.

## Conclusion

The dual-tripler scheme for broadband frequency conversion has been experimentally demonstrated. The close agreement between theory and experiment provides high confidence that the scheme will work on OMEGA and the NIF. On the basis of these results, plans are being made to convert the full OMEGA system. A similar design exists for the NIF. For both laser systems, an approximate threefold increase in bandwidth can be expected, which should result in a threefold reduction in smoothing time and correspondingly more-uniform target implosions.



TC4756,57,58,59

Figure 75.7

Sensitivity of the “11/9/9” NIF design to crystal alignment errors. In each case the solid line indicates the ideal conversion curve. The shaded area indicates the full range of possible curves (eight combinations) resulting from simultaneously applying errors of  $\pm\Delta\theta$  (external) to each of the three crystals, where  $\Delta\theta = 50 \mu\text{rad}$  [(a) and (c)] and  $25 \mu\text{rad}$  [(b) and (d)]. The results for 3.0 GW/cm<sup>2</sup>, the peak operating intensity [(a) and (b)], are not greatly different from those for 1.5 GW/cm<sup>2</sup> [(c) and (d)].

## ACKNOWLEDGMENT

This work was supported by the U.S. Department of Energy Office of Inertial Confinement Fusion under Cooperative Agreement No. DE-FC03-92SF19460, the University of Rochester, and the New York State Energy Research and Development Authority. The support of DOE does not constitute an endorsement by DOE of the views expressed in this article.

## REFERENCES

1. S. Skupsky, R. W. Short, T. Kessler, R. S. Craxton, S. Letzring, and J. M. Soures, *J. Appl. Phys.* **66**, 3456 (1989).
2. R. S. Craxton, *IEEE J. Quantum Electron.* **QE-17**, 1771 (1981).
3. D. Eimerl *et al.*, *Opt. Lett.* **22**, 1208 (1997).
4. S. Oskoui, Laboratory for Laser Energetics Report No. 277, NTIS document No. DOE/SF/19460-173 (1996). Copies may be obtained from the National Technical Information Service, Springfield, VA 22161.
5. R. S. Craxton, S. D. Jacobs, J. E. Rizzo, and R. Boni, *IEEE J. Quantum Electron.* **QE-17**, 1782 (1981).
6. R. C. Weast, ed. *CRC Handbook of Chemistry and Physics*, 58th ed. (CRC Press, Cleveland, OH, 1977), p. E-224.
7. A. Babushkin, R. S. Craxton, S. Oskoui, M. J. Guardalben, R. L. Keck, and W. Seka, *Opt. Lett.* **23**, 927 (1998).
8. A. Babushkin, W. Bittle, S. A. Letzring, A. Okishev, M. D. Skeldon, and W. Seka, in *Advanced Solid-State Lasers*, edited by C. R. Pollock and W. R. Bosenberg, OSA Trends in Optics and Photonics Series, Vol. 10 (Optical Society of America, Washington, DC, 1997), pp. 106–108.
9. W. L. Smith and T. F. Deaton, *Laser Program Annual Report 1979*, Lawrence Livermore National Laboratory, Livermore, CA, UCRL-50021-79, 2-209 (1980).